The phase transition sequence in tetramethylammonium cadmium chloride (TMCC): $[N(CH_3)_4]CdCl_3$

1997 J. Phys.: Condens. Matter 9 3399

(http://iopscience.iop.org/0953-8984/9/16/012)

J. Phys.: Condens. Matter **9** (1997) 3399–3415. Printed in the UK PII: S0953-8984(97)79788-1

The phase transition sequence in tetramethylammonium cadmium chloride (TMCC): $[N(CH_3)_4]CdCl_3$

J Díaz-Hernández†, G Aguirre-Zamalloa†, A López-Echarri†,
I Ruiz-Larrea‡, T Breczewski‡ and M J Tello†

† Departamento de Física de la Materia Condensada, Facultad de Ciencias, Universidad del País Vasco (UPV/EHU), Apartado 644, Bilbao, Spain

‡ Departamento de Física Aplicada II, Facultad de Ciencias, Universidad del País Vasco (UPV/EHU), Apartado 644, Bilbao, Spain

Received 21 November 1996

Abstract. The structural phase transitions in $[N(CH_3)_4]CdCl_3$ were investigated by means of adiabatic calorimetry and thermal expansion measurements. Two phase transitions have been studied on cooling and on heating at about 104 K and 118 K. The shapes of the observed specific heat anomalies, as well as the existence of thermal hysteresis, confirm the first-order character previously assigned to these phase transitions. From the experimental data and the harmonic specific heat obtained from the known frequencies of the vibrational modes, a calculation of the Grüneisen parameter as a function of the temperature is also given. Finally, the suitability of different Landau potentials for the two phase transitions is briefly discussed.

1. Introduction

In the field of what is known as quasi-one-dimensional materials, there has been considerable interest in compounds with the common chemical formula $[N(CH_3)_4]MX_3$, where M is a divalent metal such as Mn, Zn, Cd, and Hg, and X is a halogen [1]. Many of these compounds exhibit successive structural phase transitions which are associated with the reorientational dynamics of the tetramethylammonium groups, $[N(CH_3)_4]$ (hereafter TMA) [2–6]. Recently, a considerable effort has been made both in experimental and theoretical studies in order to achieve an understanding of the dynamical behaviour of these TMA groups, since they are mainly responsible for the order–disorder phase transitions observed. At room temperature, these compounds have an isomorphous hexagonal structure (space group $P6_3/m$ and $Z = 2$ formula units per primitive unit cell). These compounds contain infinite linear chains of face-sharing MX_6 octahedra ($\cdots$ M–X_3–M–$X_3\cdots$) running parallel to the c-axis. The TMA groups are orientationally disordered and occupy the space between the MX_6 chains [7]. Tetramethylammonium manganese chloride, $[N(CH_3)_4]MnCl_3$ (commonly abbreviated as TMMC), is perhaps the most extensively studied compound of this group, principally because of its quasi-one-dimensional magnetic properties.

Tetramethylammonium cadmium chloride, $[N(CH_3)_4]CdCl_3$ (TMCC), has also received much attention, and has been extensively investigated by means of several techniques such as Raman scattering [2, 3, 5, 8], x-ray diffraction [2, 3, 9], EPR [10], Brillouin scattering [6], NMR [4], thermal expansion [11], specific heat [12], and dielectric and ultrasonic measurements [1, 3]. At room temperature, TMCC crystallizes in a hexagonal $P6_3/m$

0953-8984/97/163399+17$19.50

structure with $Z = 2$ (phase I). The lattice constants for this crystal are $a_0 = 9.138$ Å, $c_0 = 6.723$ Å, and Cd–Cl = 2.644 Å [2, 3, 13].

At high temperature, TMCC exhibits a prototype structure with space group $P6_3/mmc$ and $Z = 2$ (the parent phase I′). The phase transition from phase I′ ($P6_3/mmc$) to phase I ($P6_3/m$), at about $T = 400$ K, is found to be of second order. Both phases exhibit orientational disorder of the TMA groups, coupled to translational disorder of the $CdCl_3$ octahedral chains [5, 6]. Additionally, TMCC presents two low-temperature structural phase transitions. The first one, taking place at $T = 118$ K, connects the disordered hexagonal phase (I) to an ordered monoclinic phase (II) with space group $P2_1/m$ and $Z = 2$. In this phase three types of domain characteristic of the ferroelastic phase transition have been found. The second transition, at 104 K, leads to another monoclinic phase (III), with space group $P2_1/b$ and $Z = 12$ [9]. The unit cell of phase (III) is related to that of phase (I) by a doubling of the lattice constant along the *b*-axis, together with a trebling of the lattice constant along the *c*-axis ($a_{III} = a_I, b_{III} = 2b_I, c_{III} = 3c_I$). These two phase transitions are of first order [3, 5, 8, 9].

In addition, another structural phase transition has been reported to occur at about 150 K [2, 6]. However it was not confirmed by any further measurement, so its existence remains unclear. Thus, the following phase transition sequence has been established at normal pressure:

$$\begin{array}{ccccccccc} \text{I}' & & 400\ \text{K} & & \text{I} & & 118\ \text{K} & & \text{II} & & 104\ \text{K} & & \text{III} \\ P6_3/mmc\,(Z=2) & \longleftrightarrow & & & P6_3/m\,(Z=2) & \longleftrightarrow & & & P2_1/m\,(Z=2) & \longleftrightarrow & & & P2_1/b\,(Z=12). \end{array}$$

On the other hand, Peercy *et al* [3], Couzi and Mlik [14], and Gesi [1] have discussed the relationship between various TMMC-like compounds. The equivalent phases present in TMMC, TMMB, and TMCC strongly suggest the possibility of finding a unified picture of the phase transition sequences in TMMC-like compounds, as was found for the $[N(CH_3)_4]_2MX_4$-type compounds. However, the variety of the structures appearing in the low-temperature ordered phases indicates that these relationships may not be simple. Also, detailed structural knowledge of the low-temperature monoclinic phases of TMCC is still lacking. Therefore, this work is presented as a contribution to establishing the unified description of the whole family on better experimental grounds.

In this work we present calorimetric and dilatometric studies of the TMCC compound in the temperature range from 60 K to 300 K, especially around the transitions interval. Up to now, reported calorimetric data have been limited to temperatures below 52 K [12]. Our specific heat and thermal expansion measurements confirm that the TMCC compound shows two first-order phase transitions in this temperature range. These results permit us to verify the order–disorder character assigned to these phase transitions. We also discuss the problems related to the Landau-type description of TMCC in the framework of a general model for this family of compounds.

2. Experimental procedure

Colourless TMCC single crystals in the form of prisms elongated along the *c*-axis were grown by the dynamic method at 305 K from saturated aqueous solution prepared with stoichiometric amounts of $[N(CH_3)_4]Cl$ and $CdCl_2$. Their chemical composition was confirmed by atomic spectroscopy.

Specific heat measurements from 60 K to room temperature have been performed using an automatic adiabatic calorimeter described in reference [15]. We have used a powder sample of TMCC to fill the calorimeter vessel. This vessel was also filled with helium gas

at low pressure to favour a good thermal equilibrium after each heating period. As we have described in previous works, two different methods were used to measure the specific heat in this range: discontinuous heating (pulse) and continuous heating (thermogram) techniques. Both methods give an accuracy better than 0.1% for the specific heats obtained.

Thermal expansion of TMCC was measured using a standard dilatometer in dynamic conditions, in the temperature range from 80 K to 300 K. Colourless single crystals in the form of prisms with dimensions of about $1 \times 1 \times 3$ cm^3 have been used. Various cooling and heating measurements with rates from 1 °C min^{-1} to 10 °C min^{-1} were made along the c- and a-axes.

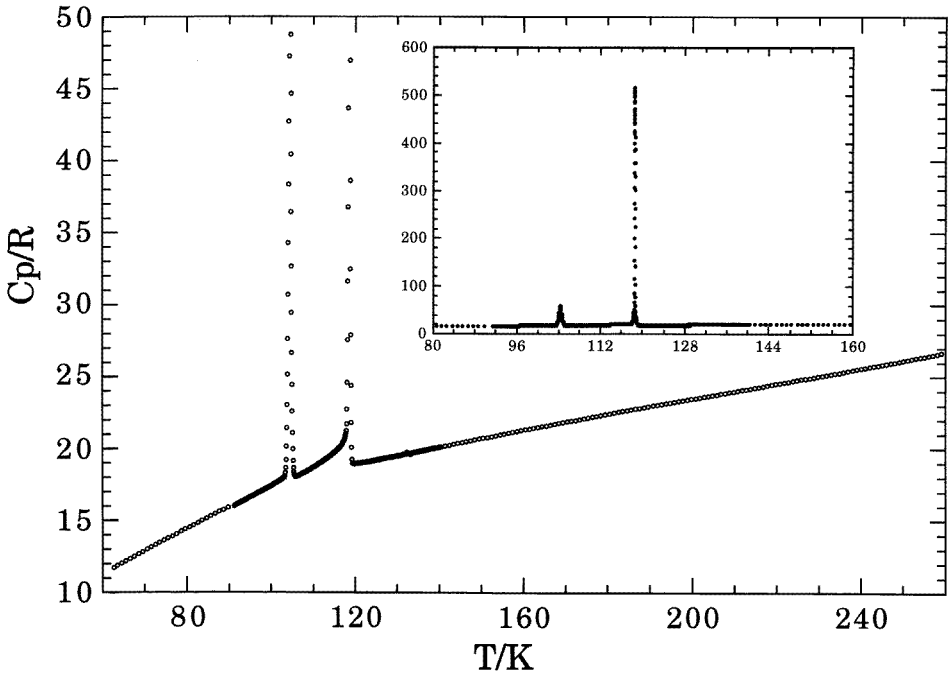

Figure 1. The specific heat of TMCC from 60 to 260 K showing two first-order phase transitions at 104.2 K ($C_p = 80R$) and 118.6 K ($C_p = 520R$). The experimental data were obtained by the pulse technique, and from dynamic thermograms with heating rates between 1.5 and 2.8 K h^{-1}.

3. Results and discussion

The experimental specific heat results are presented in figure 1. As expected, two phase transitions are found between 100 and 120 K. In order to obtain a better definition of the specific heat curve in this temperature range, various thermograms were obtained in intervals ranging from 80 K to 107 K, 116 K to 123 K, and 80 to 123 K, with heating rates varying between 1.5 and 2.8 K h^{-1}. As stated above, two specific heat peaks appear, at 104.2 K and 118.6 K. The apparent sharpness of the C_p-curve clearly indicates the first-order nature of these phase transitions.

In order to determine the values of the thermodynamic functions associated with these phase transitions ('excess' quantities), an adequate estimation of the base-line is required to separate the contribution of the phase transition mechanisms from the remaining

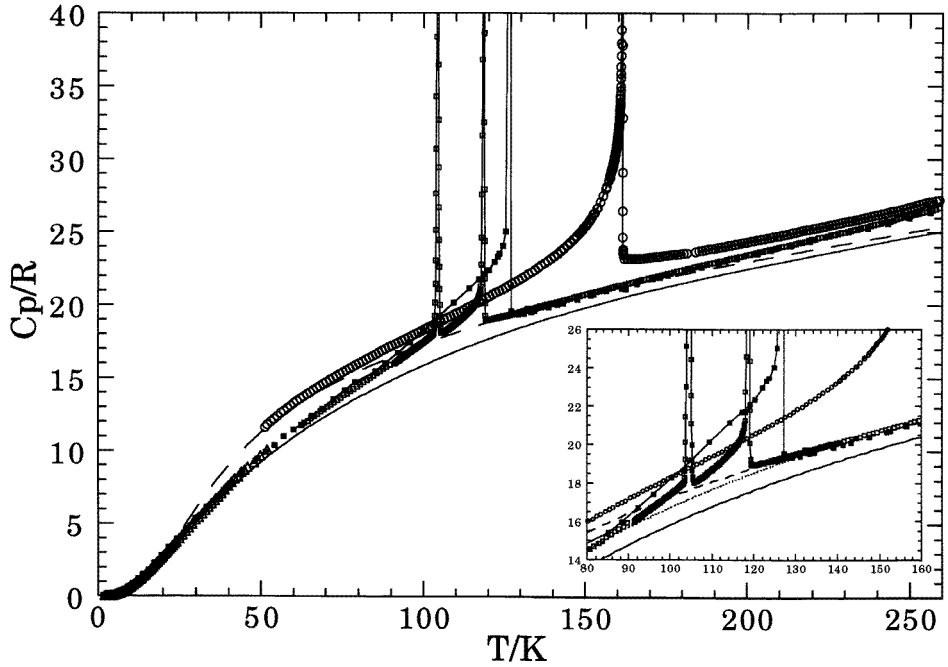

Figure 2. The specific heat of: TMCC □ (present work); TMMC, ■ [19]; and TMCB, ○ [28], around the phase transition regions. Below 52 K we have plotted the values reported by de Jonge *et al* [12] for TMCC (△). The continuous line and the dashed line are the harmonic lattice contributions to the specific heat of TMCC and TMCB respectively. In the inset, the common base-line (the dotted line) used for the calculation of the phase transition thermodynamic functions of the chloride crystals is also plotted.

contributions of the crystal lattice.

Earlier, the specific heat of the related crystals $[N(CH_3)_4]MnCl_3$ (TMMC) and $[N(CH_3)_4]CdBr_3$ (TMCB) was reported [12, 16–19]. In addition, specific heat data for TMCC and TMMC below 52 K were published in references [12] and [12, 17, 19] respectively. Where the numerical C_p-data were also included in the works cited, we can compare the behaviour of this quantity for these compounds as a function of the temperature. All of these measurements have been plotted together in figure 2. Leaving aside the anomalies associated with the phase transitions, an excellent agreement is found for the normal specific heat of TMCC and TMMC over a wide temperature range. Indeed, our present measurements for TMCC agree very nicely with the low-temperature data reported for this crystal [12]. On the other hand, the specific heats of the three compounds attain similar values for $T > 160$ K, above the phase transition undergone by TMCB. As will be seen later, the higher specific heat values which TMCB shows below this temperature are easily explained by the presence of lower frequencies in its vibrational spectrum. However, a corresponding-states law can be applied to the specific heat of TMCB in order to fit these data to the results for the chloride compounds (TMCC and TMMC). An empirical factor $f = 1.16$ for the temperature re-scaling of TMCB leads to the best fit for all three sets of specific heat data. As a consequence, a common specific heat base-line can be easily drawn. Therefore, the excess specific heat ΔC_p and, consequently, the values of the thermodynamic functions for the two phase transitions of TMCC and that of TMMC can be worked out by

subtracting this base-line from the measured C_p. The corresponding values for the II $\leftrightarrow$ III phase transition in TMCC at 104 K were obtained by a simple extrapolation of the C_p-curve on both sides of the peak. The values for the excess thermodynamic functions of TMCC across both transitions, obtained by numerical integration, are displayed in table 1.

Table 1. Values of the excess thermodynamic functions of TMCC across the two transitions. These values have been calculated by numerical integration using the experimental data, and the base-lines constructed as explained in the text.

	$\Delta H/RK$	$\Delta S/R$
$T = 104.5$ K	35.17	0.339
$T = 118.6$ K	115.71	0.985

The entropy of the phase transition at 118.6 K in TMCC is close to the value reported by Dunn *et al* [19] for TMMC at 126 K ($\Delta S/R = 1.024$) and this result remains unchanged when we use the common base-line obtained for both compounds. However, care must be taken with the results for TMMC as the experiments were performed only by means of the adiabatic pulse method, which can lead to significant errors when latent heat is present. In both cases the phase transition entropy approximates to $R \ln 3$, far below the value exhibited by the TMCB phase transition at $T = 156$ K ($\Delta S \approx R \ln 8.8$). This latter value was calculated within the Nernst–Lindemann approximation [20, 21], and may be somewhat overestimated.

The lattice harmonic contribution to the specific heat can be determined by means of the lattice mode frequencies obtained from Raman and infrared measurements on TMCC [5, 8]. The frequencies of the inactive modes have been estimated from data obtained from related compounds [16, 22].

We have used these spectroscopic data to calculate the contributions adding up from the lattice modes and the internal modes of the TMA groups. From group theory applied to the organic tetrahedron (including the four methyl groups) we can obtain the decomposition of the 45-dimensional vibrational representation as a sum of the irreducible group representations, which accounts for the TMA internal modes:

$$\Gamma_{45} = 3\mathrm{A}_1(1) + 4\mathrm{E}(2) + 4\mathrm{T}_1(3) + 7\mathrm{T}_2(3) + \mathrm{A}_2(1).$$

A similar analysis applied to the space group $P6_3/m$ (point group $6/m$) shows the 36-dimensional representation at $\boldsymbol{k} = 0$, describing the external (translational and rotational) modes of the organic tetrahedron and inorganic octahedron, for $Z = 2$:

$$\Gamma_{36} = 3\mathrm{A}_\mathrm{g}(1) + 2\mathrm{B}_\mathrm{g}(1) + 2\mathrm{E}_{1\mathrm{g}}(2) + 3\mathrm{E}_{2\mathrm{g}}(2) + 3\mathrm{A}_\mathrm{u}(1) + 4\mathrm{B}_\mathrm{u}(1) + 4\mathrm{E}_{1\mathrm{u}}(2) + 3\mathrm{E}_{2\mathrm{u}}(2).$$

Table 2 summarizes the frequency assignments used to construct the harmonic specific heat. In general, the values assigned to TMCC are similar to those found for TMMC [5, 8] and TMCB (see [16] and references therein, [23]), with only slight differences in the low part of the spectrum which are more pronounced for this last crystal. As expected, the frequencies associated with the bending and stretching modes of the Br–Cd bonding are smaller than in the case of Cl–Cd or Cl–Mn, as a result of the mass differences between the two halogen ions. Different frequencies for the external movements of the molecular groups should also be noted. In the upper extreme of the vibrational spectrum, all of the internal frequencies of the tetramethylammonium groups are practically the same in all of these compounds, because the corresponding modes are not coupled with the lower frequencies associated with the translational and rotational modes of the molecular groups. It should be

Table 2. Frequency assignments for TMCC and TMCB normal modes. (a) Translational and rotational modes of the TMA and BX_3 molecular groups. * represents estimated values obtained from related compounds. (b) Tetramethylammonium internal modes.

(a)

	Frequency (cm^{-1})			
Symmetry	TMCC	TMCB	Assignment	Degeneracy
A_g	248	156	ν (chains)	1
A_g	80	40	R (chains)	1
A_g	50	70	R (TMA)	1
B_g	200*	130	ν (chains)	1
B_g	50*	60	T (TMA)	1
E_{1g}	100	80	δ (chains)	2
E_{1g}	50*	70	R (TMA)	2
E_{2g}	164	56	T (TMA)	2
E_{2g}	118	90	δ (chains)	2
E_{2g}	74	105	δ (chains)	2
A_u	$\omega_D = 60$*	40	Acoustic	1
A_u	50	60	T (TMA)	1
A_u	170	130	ν (chains)	1
B_u	150*	130	ν (chains)	1
B_u	120*	90	δ (chains)	1
B_u	100*	105	δ (chains)	1
B_u	50*	70	R (TMA)	1
E_{1u}	$\omega_D = 50$*	50	Acoustic	2
E_{1u}	220*	105	δ (chains)	2
E_{1u}	135*	90	δ (chains)	2
E_{1u}	80*	60	R (TMA)	2
E_{2u}	170*	130	ν (chains)	2
E_{2u}	120*	90	δ (chains)	2
E_{2u}	50*	70	R (TMA)	2

(b)

Symmetry	Frequency (cm^{-1})	Assignment	Degeneracy
A_1	2922	ν_s (CH_3)	1
A_1	755	ν_s (C_4N)	1
A_1	1410	δ_s (CH_3)	1
A_2	220	τ (CH_3)	1
E	2955	ν_a (CH_3)	2
E	1171	ν_a (CH_3)	2
E	366	δ_s (C_4N)	2
E	1450	δ_a (CH_3)	2
F_1	1486	δ_a (CH_3)	3
F_1	1290	ρ (CH_3)	3
F_1	955	ν_a (CH_3)	3
F_1	3026	ν_d (CH_3)	3
F_1	320	τ (CH_3)	3
F_2	2922	ν_s (CH_3)	3
F_2	3026	ν_a (CH_3)	3
F_2	1486	δ_a (CH_3)	3
F_2	1410	δ_s (CH_3)	3
F_2	1290	ρ (CH_3)	3
F_2	455	δ_a (C_4N)	3

pointed out that the harmonic specific heat in the temperature range in which the various phase transitions of these crystals are present is governed by the normal lattice modes related to the internal movements of the TMA group and to the bending and stretching modes of the metal–halogen bonds. These frequencies extend from 100 cm^{-1} to 1500 cm^{-1}. The contributions to the specific heat of the lower-frequency modes rapidly attain their saturated values (given by the Dulong and Petit law) at relatively low temperatures, avoiding errors in the estimated specific heat due to incorrect frequency assignments. In the case of TMCB, this saturation is reached at lower temperatures than in the chloride crystals, and this explains the higher specific heat values found in this range. However, when the complete contribution of all of these modes is finally attained, at higher temperatures, the specific heat of all three crystals must be the same, as the experiments confirm.

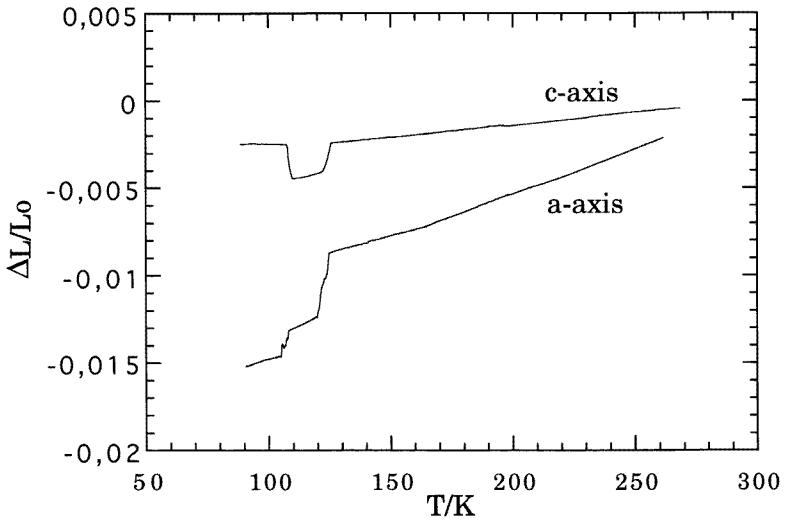

Figure 3. The thermal expansivity of TMCC along the crystallographic directions c and $a = b$. The heating rates were 10 K min^{-1}.

For the calculation of the harmonic specific heat, Einstein functions have been used for the optical modes, weighted with the corresponding degeneracies. The contribution of the three acoustic modes has been calculated with Debye functions, with estimated cut-off frequencies of about 50 cm^{-1}. The total harmonic lattice contribution for TMCC, TMMC, and TMCB is plotted in figure 2.

Figure 3 shows the dependence of the thermal expansivity of TMCC along the c- and a-axes (α_c and α_a). As all of the directions perpendicular to the c-axis are isotropic in the hexagonal phase, the experimental information permits us to retrieve the volume thermal expansion $\alpha = \alpha_c + 2\alpha_a$. However, below the hexagonal–monoclinic phase transition at 118 K, more experimental information would be required for a precise determination of the thermal expansion tensor. The measurements were performed on cooling and heating at various rates. The curves show two phase transitions at about 104 K and 118 K, and the measured thermal hystereses, not displayed on this plot, for both phase transitions, were of 6 K and 4 K, respectively. The first-order nature of the two phase transitions is also confirmed by the jump of the thermal expansion curves at the two transition temperatures, in agreement with our experimental specific heat results. As can be seen from the slopes of both curves, the thermal expansion coefficient in the isotropic directions perpendicular to

the c-axis (α_a) is very much larger than that along the c-axis (α_c). For example, at room temperature $\alpha_a \approx 4.4\alpha_c$. This result is also observed in the axial isothermal compressibilities ($K_T^a = K_T^b$ and $K_T^a \approx 5K_T^c$) along these directions in TMMC [3], and it is explained by the higher crystal stiffness along the rigid inorganic chains as compared with the small inter-chain electrostatic forces.

The behaviour of the thermal expansion around the two phase transitions is worth analysing. On heating, the III $\rightarrow$ II phase transition at 104 K is characterized by a small increase of the cell dimensions in the plane perpendicular to the c-axis. However, the cell volume remains practically unchanged due to a simultaneous contraction of the pseudo-hexagonal axis. In this situation the TMA group reorientations inside the inorganic chains are still avoided and the structure is ordered, a fact which is confirmed by Raman experiments [8, 14]. The disorder of the organic groups comes in at the I phase transition, where a noticeable increase of the cell volume (about 1%) takes place, as a result of the simultaneous expansion along the three axes. The expansion is more pronounced in the a–b plane, and the corresponding separation of the chains favours orientational disorder of the TMA groups. This fact is also supported by the higher entropy value of the II $\leftrightarrow$ I phase transition.

The anharmonic contribution to the specific heat could be established by thermodynamical procedures if full experimental data for the elastic constants and the thermal expansion coefficients of the crystal were available. In other cases, approximate rules such as the Nernst–Lindemann relation can be used [20, 21]. However, the subtraction of the harmonic specific heat (which in the following will be identified with the specific heat at constant volume, C_v) from the experimental value of C_p allows us to obtain directly the anharmonic contribution to the specific heat. In addition, the thermal expansion data permit a direct calculation of the Grüneisen parameter (Γ) and the isothermal compressibility (K_T), which describe the crystal anharmonicity as a function of the temperature.

From the thermodynamic relations

$$C_p - C_v = \frac{TV\alpha^2}{K_T} \tag{1}$$

and

$$\Gamma = \frac{\alpha V}{K_T C_v} \tag{2}$$

where V is the molar volume, and α is the volume thermal expansivity, we obtain Γ and K_T as functions of the experimental data. For instance,

$$\Gamma = \frac{C_p - C_v}{T\alpha C_v}. \tag{3}$$

Combining these data with C_p and C_v, in figure 4 we show the behaviour of the Grüneisen parameter and the isothermal compressibility for TMCC. Above the phase transition temperature range, Γ progressively attains a constant value. At 290 K, $\Gamma = 2.26$, which is a typical value for many solids at room temperature. At this temperature, K_T is 3.47×10^{-11} Pa^{-1}, which compares well with the result obtained for isomorphous TMMC from the axial compressibilities [3]: $K_T = 2K_T^a + K_T^c = 4.42 \times 10^{-11}$ Pa^{-1}.

Moreover, the phase transition sequence exhibited by the isomorphous compound TMMC at about 2.5 kbar is found to be the same as that of TMCC at atmospheric pressure [3, 14]. This hint led some authors to propose a generalized pressure–temperature phase diagram for all of the compounds of the family with the exception of TMCB [14, 24], similar to the phase diagram describing the various phase transition sequences for the $(TMA)_2BX_4$ compounds [25, 26].

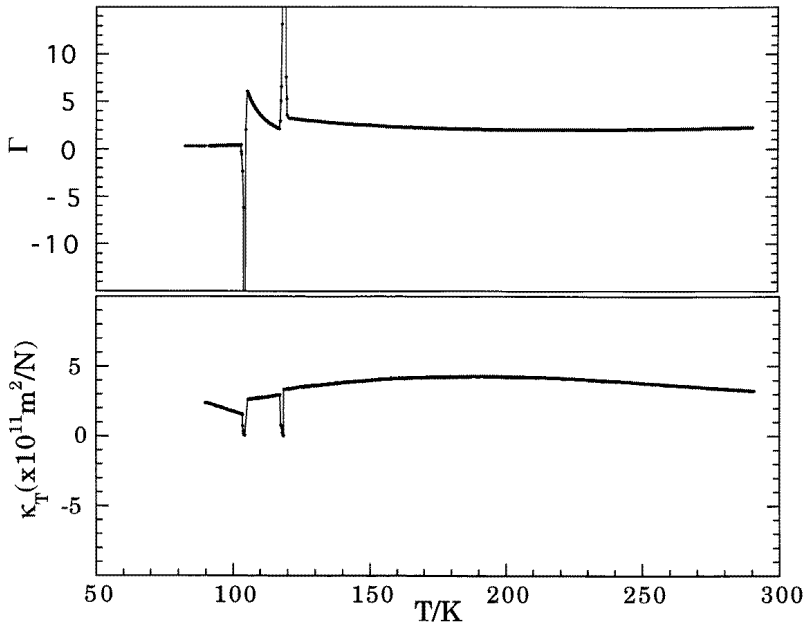

Figure 4. The Grüneisen parameter (Γ) and the isothermal compressibility (K_T) for TMCC, obtained from the experimental specific heat and the thermal expansion measurements.

Taking the reported values for the lattice constants under hydrostatic pressure from Peercy *et al* [3] we can calculate the size reduction of the TMMC unit cell from atmospheric pressure ($V = 470.95$ Å^3) to 2.5 kbar ($V = 465.73$ Å^3). Throughout this pressure range, the cell volume of TMMC remains smaller than that of TMCC at atmospheric pressure ($V = 486.3$ Å^3). This result is supported by the fact that the covalent radius of the Cd atom is larger than that of the Mn atom.

In contrast, at atmospheric pressure, the TMMC cell dimensions in the plane perpendicular to the *c*-axis ($a = b = 9.151$ Å) are larger than the ones for TMCC ($a = b = 9.139$ Å). In this situation, the inorganic chains along the *c*-axis are closer in TMCC, and the motions of the TMA groups between the chains are more strongly hindered. As the I ↔ II phase transition is associated with the TMA ordering, it follows that the transition temperature is expected to increase with pressure.

When pressure is applied to TMMC, the lattice parameters *a* and *b* are considerably reduced due to the low linear compressibility on this plane, and progressively approach the values for TMCC. This effect can explain the fact that under high pressure (the threshold value being about 1 kbar [8]), TMMC shows the same phase transition sequence as TMCC at atmospheric pressure. This has been confirmed by different experiments [3, 14].

The orientational ordering of the TMA groups is also established for the hexagonal–hexagonal ferroelectric phase transition of TMCB at 156 K [27, 28]. In this case, the cell constant '*a*' is larger ($a = 9.388$ Å) than in the chloride crystals. However, calculations show that the separation of the inorganic $\cdots Br_3$–Cd–Br_3–Cd$\cdots$ chains is even smaller, resulting from the larger size of the bromide ions. This can explain the higher transition temperature of TMCB, and perhaps the large value for the transition entropy. These two features are also observed for $(TMA)_2BX_4$ compounds when the bromide–

chloride substitution takes place. However, further thermodynamic information (e.g. specific heat measurements under pressure) would be required for a deeper understanding of the equivalence between ion substitution and applied pressure.

4. Discussion of the symmetry properties and Landau potentials for TMCC

The analysis of symmetry properties and the description of the different excess magnitudes within the framework of the Landau theory has already been given for the (ferroelectric) TMCB [22, 28, 29] and (ferroelastic) TMMC [30] compounds belonging to the family of TMCC, with relative success.

Whereas the symmetry properties of the principal order parameters (POP, as opposed to secondary OP) driving the transitions in all of these compounds are well known [31], the physical mechanisms at play are still very complex. Usually these POP, pertaining to different points of the Brillouin zone, consist of the so-called pseudo-spin coordinates embodying the reorientational dynamics of the TMA groups [32], coupled (linearly or not) with components of the stress tensor (ferroelastic transitions) [33] or polarization vector components (ferroelectric transitions) [34]. Further displacive contributions arising from the rotations or translations of the MX_6 octahedra chains cannot be neglected in general [8, 9].

The two phase transitions of TMCC are markedly distinct, and will be dealt with separately in the discussion that follows for the sake of clarity.

4.1. The I ↔ II *transition*

At a temperature of about $T \approx 118$ K and ambient pressure, the following first-order proper ferroelastic phase transition takes place in TMCC [9]:

$$\underset{\text{phase I}}{P6_3/m\ (Z=2)} \quad \longleftrightarrow \quad \underset{\text{phase II}}{P2_1/m\ (Z=2)}.$$

Raman scattering studies [8, 14] have shown, first, strong evidence in favour of a completely ordered phase II, and second, the total absence of soft-mode behaviour, thus confirming the pure order–disorder character of the transition. From symmetry considerations it can be shown that only one POP (η) is involved in this transition [30, 31]; also, the presence of the cubic invariants in the potential expansion forces the transition to be of first order, in complete agreement with the experimental results. As regards the nature of the order parameters, they include pseudo-spin coordinates issuing from some suitable Frenkel model (two-, three- or six-well models) [27, 28, 35], bilinearly coupled to the $(e_1 - e_2, e_6)$ stress tensor components of $\Gamma_5^+\Gamma_6^+/E_{2g}$ symmetry [36] (pseudo-proper ferroelastic). This latter fact has been nicely demonstrated by the marked softening affecting the evolution of the C_{11} and C_{66} elastic constants in the hexagonal phase near the transition temperature [6, 8], which closely resembles the behaviour shown by the related ferroelastic compound TMMC [8, 37]. In fact, the elastic data are slightly problematic: the C_{66}-data were obtained with the help of ultrasonic techniques, and come from an unpublished preliminary account by Braud *et al* [8]. On the other hand, the C_{11}- (and C_{33}-) measurements were obtained by means of the Brillouin scattering technique [6], and though the raw data look quite correct, the discussion given by Levola *et al* (for instance, altogether neglecting the first-order character of the transition) is unsound and ought to be revised [30, 31].

Details about the connection between the different Frenkel models and the pseudo-spin coordinates can be found in references [14, 28, 31, 32]. Although the six-well (6W) model has proved to be the best suited for describing the disordered configuration of the TMA

groups in the compounds TMMC [38] and TMCB [27], it is nonetheless unable by itself to reach a completely ordered state of the TMA groups in phase II of TMCC. Therefore, if the ordering process is to be led by this model, it has to be necessarily assisted by large-amplitude anharmonic librations of the TMA groups (the pseudo-spin–phonon coupling mechanism), resulting in a reconstructive transition, anyway [27, 28, 31]. Actually, if we assume that phase II is completely ordered, as spectroscopic data seem to indicate, we can hardly reconcile the value of the excess entropy jump across the first transition (i.e. $\Delta S \approx R \ln 2.68$; see table 1), calculated with the given base-line, with the theoretical value predicted by the 6W model ($\Delta S = R \ln 6$). These considerations must be handled with great care [39], and by no means do they imply that the 6W model is automatically ruled out; indeed, for the related compound TMMC, whilst the calorimetric results mentioned above [19] are clearly in favour of a 3W model, the recently achieved structural resolution of both phases has shown beyond doubt that the 6W model gives a better description of the orientational disorder [38]. Further, more selective experiments are needed to decide about the nature of the orientational disorder in phase I in TMCC.

The Landau potential describing this I $\leftrightarrow$ II transition, developed to the lowest order, has been calculated elsewhere in detail [30, 31]. This potential comprises the contributions from the POP itself, from the elastic terms and from the interaction between them, and has been used to predict the thermal evolution of the elastic constants in the hexagonal phase only, since the domain pattern of the ferroelastic phases makes their observation impossible. In practice, it turns out that the 'effective' or 'renormalized' potential to be compared with the actual C_p-measurements is essentially a simple 234 classical potential [31].

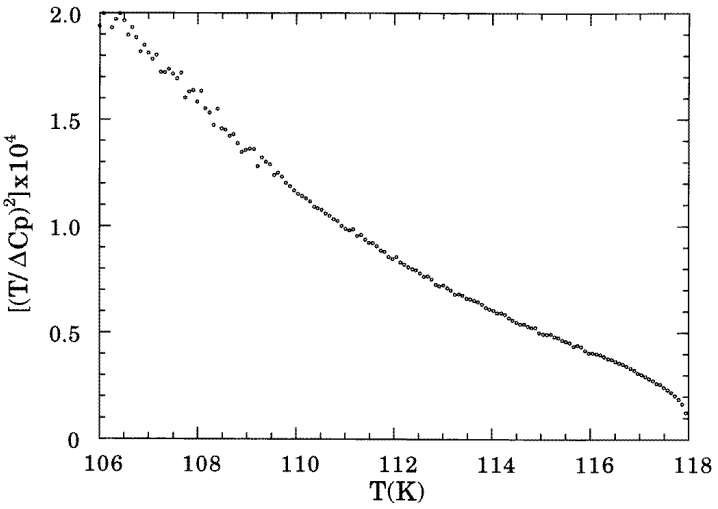

Figure 5. A plot of $(T/\Delta C_p)^2$ versus temperature obtained from the experimental specific heat and the base-line, as explained in the text.

It should be emphasized that the base-line, however carefully estimated, is arbitrary to a certain extent. Hence, the excess quantities are not absolute, but rather depend on the method of construction explained above. Bearing this in mind, we have compared the experimental calorimetric results with the predictions of such a development. There exist several highly significant 'test' plots which can reveal the different scenarios [28, 33]. One such is the $(T/\Delta C_p)^2$ versus T plot: whenever this function is convex (negative

curvature), the transition will be of first order because of the presence of a third-order invariant; otherwise, if this test quantity appears to be a straight line, the transition is first order because of a negative fourth-order term (see the appendix). We have thus plotted in figure 5 the quantity $(T/\Delta C_p)^2$ for TMCC in the temperature range between the two transitions. It displays an unambiguous concave pattern (positive curvature), analogous to the one found for the isomorphous compound TMCB [28]. At this stage, these results deserve some thought because, as it stands, simple 2346 potentials (i.e. including η^2-, η^3-, η^4- and η^6-terms) are unable to explain this behaviour (see the appendix).

Admittedly, we can modify the 2346 potentials in a number of ways, by relaxing some of the normally accepted hypotheses so as to obtain the ubiquitous concave pattern. This can be achieved most easily by formally adding another asymmetric term, say the fifth-order term, to the limited development. The concave behaviour will result if some trade-off between the third- and fifth-order terms is respected. Anyway, the need for extending the development at least to the sixth order seriously increases the complexity of the treatment, for higher-order coupling terms have to be taken into account. As a result, the expression for the free-energy ends up depending upon so many unknown parameters that their fitting to the ensemble of experimental data provides a less significant test of the overall adequacy of the Landau description to the data [34].

There is still another possibility. Less simply, this behaviour can be reproduced with developments limited up to the fourth order, by assuming a non-linear behaviour of the second-order coefficient, or even assuming that the 'constant' b-coefficient eventually depends on T [22]. These odd effects in the effective potential may arguably result—given the proximity of the two transitions—from the coupling to the other POP, on account of various non-Landau precursor effects. This point has to be explored further.

In order to resolve this dilemma, we think it necessary to perform some complementary and independent measurements to gain additional insight into the transition mechanisms. Structural studies of both ordered and disordered phases, emphasizing the study of the TMA groups and the re-determination of the evolution of the elastic constants C_{66} and C_{11} in the hexagonal phase with the help of ultrasonic techniques, have the utmost importance.

4.2. The II $\leftrightarrow$ III *transition*

The situation in the lowest-temperature phase is much more complex. To begin with, let us recall that phase III exhibits the doubling and trebling of the lattice parameters a and c respectively, with respect to those of the hexagonal unit cell (a sixfold unit-cell volume increase). At a temperature of nearly $T \approx 104$ K and ambient pressure, the following first-order isoclass phase transition takes place in TMCC [1, 9]:

$$\underset{\text{phase II}}{P2_1/m\ (Z=2)} \quad \longleftrightarrow \quad \underset{\text{phase III}}{P2_1/b\ (Z=12)}.$$

First, some general remarks about the transition follow, and thereafter we will very briefly survey the problems that arise when we try to proceed with the Landau approach. A report dealing specifically with the construction of the generalized phase diagram is in preparation [40]. Clearly, the fact that these space groups are group–subgroup related enables one to study the transition within the framework of the Landau theory. Also, the lowest-temperature symmetry group conveys an important reduction of translational symmetry, which necessarily involves the appearance of many antiphase domains; eventually, these domains can very seriously entangle its structural resolution [38]. Finally, this transition taking place between two orientationally ordered phases certainly precludes the POP from being a pseudo-spin coordinate. The nature of these POP remains to be elucidated.

Table 3. (a) Symmetries of the principal order parameters η, ξ, and q, along with examples of transitions where these POP intervene. (b) A description of the different phases of TMCC in terms of the three order parameters η, ξ, and q (see the text).

(a)

Symmetry	Phase transition explained	Compound
$\eta(\Gamma_5^+\Gamma_6^+/E_{2g})$	$P6_3/m$ $(Z=2) \leftrightarrow P2_1/b$ $(Z=4)$	TMMC [31]
$q(\Delta_2\Delta_3/E_1)$	$P6_3/m$ $(Z=2) \leftrightarrow P6_1$ $(Z=6)$	TMCB [29]
$\xi(M_1^-/A_u)$	$P6_3/m$ $(Z=2) \leftrightarrow P2_1/b$ $(Z=4)$	TMMC [31]

(b)

Phase	(η_1, η_2)	(ξ_1, ξ_2, ξ_3)	(q_1, q_2, q_3, q_4)	Space group
I	$\eta_1, \eta_2 = 0$	$\xi_1 = \xi_2 = \xi_3 = 0$	$q_1 = q_2 = q_3 = q_4 = 0$	$P6_3/m$ $(Z=2)$
II	$\eta_1 \neq 0, \eta_2 \neq 0$	$\xi_1 = \xi_2 = \xi_3 = 0$	$q_1 = q_2 = q_3 = q_4 = 0$	$P2_1/m$ $(Z=2)$
III	$\eta_1 \neq 0, \eta_2 \neq 0$	$\xi_1 \neq 0, \xi_2 = \xi_3 = 0$	$q_1 = q_2 \neq 0, q_3 = q_4 \neq 0$	$P2_1/b$ $(Z=12)$
Virtual phase	$\eta_1 \neq 0, \eta_2 \neq 0$	$\xi_1 = \xi_2 = \xi_3 = 0$	$q_1 = q_2 \neq 0, q_3 = q_4 \neq 0$	$P2_1/m$ $(Z=6)$

As mentioned above, we have worked out Landau potentials able to describe satisfactorily the phase transitions taking place in TMCB [28] and TMMC [30] independently. Now, the Landau potentials required to describe the phase transitions in TMCC (and the II $\leftrightarrow$ III transition in particular) are much more involved. In a way, solving the problem for TMCC amounts to giving a complete picture for the whole family; TMCC is, so to speak, the cornerstone of the unified description, and we claim that it should certainly not be analysed in isolation. In fact, three POP of different symmetries, $\eta(\Gamma), q(\Delta)$, and $\xi(M)$ (see table 3), have been shown to take account of the ensemble of phase transitions occurring in these compounds [28, 31], and—what is most remarkable—all three come into play when one tries to explain the stabilization of phase III of TMCC. This scheme is the most natural that can be advanced, since it supports the existence of phase III, and all of the intermediate phases with $Z = 2, Z = 4$, and $Z = 6$ appearing in the compounds of the family, with no need to introduce any supplementary OP. Another hypothesis has been proposed [31], suggesting that the lattice instability takes place at the point U, $(0, \frac{1}{2}, \frac{1}{3})$, of the Brillouin zone [36]. But this would require the introduction of a new OP able to describe the I $\leftrightarrow$ III direct transition with the absence of any intermediate phase, a process that has never been observed experimentally. We think that such a mechanism is not very realistic.

Also, symmetry arguments lead naturally to a proposal of the existence of an intermediate hypothetical phase resulting from the interaction of the POP η and q: $P2_1/m$ $(Z = 6)$ (see table 3). Even if this 'virtual' phase has not been detected up to now, it appears nevertheless as an important element in the construction of a truly unified family phase diagram [40, 41].

Let us note here that the determination, within the framework of the Landau theory, of the different topologies of the phase diagrams arising from potentials allowing two interacting OP, albeit complex, can be worked through in some cases [42–44]. Now, the description of the generalized phase diagram (and, at the same cost, the description of phase III of TMCC) requires introducing at least three interacting POP. In so doing, we are disregarding the transition to the highest common para-phase $P6_3/mmc$ $(Z = 2)$ (phase I′), which takes place at such a high temperature that it can be safely disconnected from the other phases [31]. Up to now we have not written down the full potential describing

phase III, since the mathematical manipulations soon become very cumbersome; as far as we know, this painstaking procedure has never been conducted. Thus, the completion of the Landau description is still pending.

In order to complete the experimental study of this compound we propose some experiments, such as the study of solid solutions TMMB–TMCB and TMCB–TMCC, pursuing the competition between the OP η and q and, as mentioned above, the completion of the structural study of the low-temperature ferroelastic phases. Of course, enlarging the T, P domain of study of all of the techniques should be very helpful.

5. Conclusions

From our experimental results, the following conclusions concerning the structural phase transitions occurring in TMCC can be drawn.

(1) Our specific heat and thermal expansion measurements confirm the existence of two structural first-order phase transitions at 104 K and 118 K.

(2) In our specific heat measurements, the values associated with the anomalous transition entropy change confirm the order–disorder character assigned to the phase transition at 118 K.

(3) An indirect method for estimating the anharmonic quantities such as the isothermal compressibility and the Grüneisen parameter has been used. Although these procedures might lead to noticeable errors in the final results, the order of magnitude of these quantities—hard to establish by direct measurements—is easily calculated.

(4) Moreover, the group theoretical and the still-to-be-completed Landau treatments reveal the stunning complexity inherent to these systems. More experimental data on TMCC are needed to help in establishing the full picture of this family of compounds.

(5) The phase transition at 154 K mentioned by other authors [2, 6] was not detectable in our measurements.

Acknowledgments

This work was supported by the Universidad del País Vasco (UPV/EHU) under projects 063.310-EB046/93 and 063.310-EA139/95. The authors are indebted to Professor M Couzi (University of Bordeaux I) for fruitful discussions about the phenomenological models. One of the authors (J Díaz-Hernández) gratefully acknowledges the Universidad Autónoma de Puebla and also CONACYT-México for a thesis grant.

Appendix

In this appendix the connection between the concavity of the $(T/\Delta C_p)^2$ versus T plot and the 2346-type Landau potentials will be demonstrated on general grounds. Clearly a sixth-order 2346 potential is only meaningful as long as the coefficient of the fourth-order term happens to be negative; however, in what follows we will keep our discussion general. The purpose of these calculations consists in evaluating the sign of the second derivative of this quantity with respect to the temperature, for the particular case of the 2346 potential. This kind of analysis has already been performed elsewhere for the solvable 246 and 234 potentials [28, 41]. Nevertheless the present analysis does not depend on the detailed knowledge of the solutions, but is mainly concerned with the structure of the potential itself

(let us stress here that no analytical solution in closed form is known for the 2346 potential). The 2346 excess potential can be written as

$$\Phi = \tfrac{1}{2}a\eta^2 + \tfrac{1}{3}b\eta^3 + \tfrac{1}{4}c\eta^4 + \tfrac{1}{6}d\eta^6 \tag{A1}$$

where b, c, d are constant coefficients, and we take $d > 0$. Now, following Landau, the coefficient of the quadratic term depends linearly on the temperature:

$$a(T) = \alpha(T - T_0) \qquad \text{with } \alpha > 0 \tag{A2}$$

where α is a constant. (Remark concerning the notation: in this appendix we omit altogether the Δ that usually tags excess quantities; we write Φ instead of $\Delta\Phi$, for instance.) We calculate the transition entropy and specific heat of the transition with the help of the classical expressions

$$S = -\frac{\partial\Phi}{\partial T} \qquad C_p = T\frac{\partial S}{\partial T}. \tag{A3}$$

Combining (A1)–(A3) we then get

$$\left(\frac{T}{C_p}\right)^2 = (-\alpha\eta\eta')^{-2} \tag{A4}$$

adopting the useful shorthand

$$\eta' = \frac{\partial\eta}{\partial T}.$$

As regards the true minimum of the potential, it is necessarily a local minimum, so it satisfies the following two equations:

$$\frac{\partial\Phi}{\partial\eta} = \eta(a + b\eta + c\eta^2 + d\eta^4) = 0 \tag{A5a}$$

and

$$\frac{\partial^2\Phi}{\partial\eta^2} = (a + b\eta + c\eta^2 + d\eta^4) + \eta(b + 2c\eta + 4d\eta^3) > 0. \tag{A5b}$$

From the examination of the $\eta \neq 0$ solution, corresponding to the ferroelastic phase, it can be concluded that the stability condition (A5b) requires $\mathrm{sgn}[\eta] = \mathrm{sgn}[b+2c\eta+4d\eta^3]$. Besides this, the assumption that $d > 0$ can now be justified on account of the global stability of the potential, for when high values of the saturated OP η are considered, equation (A5b) has still to be obeyed. Further, taking the derivative of equation (A5a) with respect to the temperature, we arrive at this useful expression:

$$\frac{\partial}{\partial T}(a + b\eta + c\eta^2 + d\eta^4) = 0 \Rightarrow \eta'\frac{-\alpha}{b + 2c\eta + 4d\eta^3} \tag{A6}$$

which permits us to turn into algebraic equations all of the expressions involving higher derivatives of η with respect to T. Moreover, from (A6) it nicely leads to $\mathrm{sgn}[\eta] = -\mathrm{sgn}[\eta']$ as can be expected. At this point we are now able to take the successive derivatives of $(T/C_p)^2$ with respect to T. We obtain for the ferroelastic phase

$$\left(\left(\frac{T}{C_p}\right)^2\right)' = \frac{2}{\alpha^3}\left(\frac{b}{\eta^3} - 8d\right) \tag{A7}$$

and

$$\left(\left(\frac{T}{C_p}\right)^2\right)'' = -\frac{6b}{\alpha^3}\frac{\eta'}{\eta^4}. \tag{A8}$$

Clearly we have that

$$\operatorname{sgn}\left[\left(\left(\frac{T}{C_p}\right)^2\right)''\right] = \operatorname{sgn}[-b\eta'] = \operatorname{sgn}[b\eta]. \tag{A9}$$

It is straightforward to show by inspection that the quantity $b\eta$ is always negative. If the c-coefficient were positive, the only possibly negative term—that is to say, the only term in the potential that could compete with the second-order term—would be the third-order term, which can stabilize a minimum for $\eta \neq 0$ even before the sign of the second-order term flips down. This mechanism explains the setting in of a first-order phase transition at a temperature higher than T_0, such that η has the opposite sign to b, and hence $b\eta < 0$. Next, when the c-coefficient is negative, the fourth-order term also contributes to decreasing the potential, along with the third-order one. Nevertheless, the point is that the fourth-order term is symmetric (even), so, however small the ratio b/c is, it is always the third-order—asymmetric—term which determines for the absolute minimum, and we get again $b\eta < 0$. Further, the examination of equation (A7) reveals that the quantity $(T/C_p)^2$ is, in all cases, a decreasing function of the temperature. We should not fail to mention that for the particular instance where $b = 0$ (24 and 246 potentials), the quantity $(T/C_p)^2$ gives a straight line of negative slope.

We can therefore state as a conclusion that for the 2346 Landau potentials the test $(T/C_p)^2$ quantity is always a decreasing convex (negative-curvature) or straight (zero-curvature) function of the temperature.

References

[1] Gesi K 1992 *Ferroelectrics* **137** 209
[2] Peercy P S and Morosin D 1971 *Phys. Lett.* **36A** 409
[3] Peercy P S, Morosin D and Samara G A 1973 *Phys. Rev.* B **7** 3378
[4] Tsang T and Utton D B 1976 *J. Chem. Phys.* **57** 3780
[5] Mlik Y and Couzi M 1982 *J. Phys. C: Solid State Phys.* **15** 6891
[6] Levola T and Laiho R 1988 *Solid State Commun.* **66** 557
[7] Stucky G D 1968 *Acta Crystallogr.* B **24** 330
[8] Braud M N, Couzi M, Chanh N B and Gomez-Cuevas A 1990 *J. Phys.: Condens. Matter* **2** 8229
[9] Braud M N, Couzi M, Chanh N B, Courseille C, Gallois B, Hauw C and Meresse A 1990 *J. Phys.: Condens. Matter* **2** 8209
[10] Yu Jiang-Tsu, Liu Kuo-Tung and Jeng Yng-Huey 1994 *Solid State Commun.* **89** 543
[11] Kabrizi M and Steinitz M O 1989 *Solid State Commun.* **6** 599
[12] De Jonge W J M, Swuste C H W, Kopinga K and Takeda K 1975 *Phys. Rev.* B **12** 5858
[13] Morosin B 1972 *Acta Crystallogr.* B **28** 2303
[14] Couzi M and Mlik Y 1986 *J. Raman Spectrosc.* **17** 117
[15] Zubillaga J, Lopez-Echarri A and Tello M J 1985 *Thermochim. Acta* **92** 283
[16] Igartua J M, Aguirre-Zamalloa G, Ruiz-Larrea I, Couzi M, Lopez-Echarri A and Breczewski T 1994 *J. Thermal Anal.* **41** 1211
[17] Vis B, Chau C K, Weinstock H and Dietz R E 1974 *Solid State Commun.* **15** 1765
[18] Dietz R E, Walker L R, Hsu F S L, Haemmerle W H, Vis B, Chau C K and Weinstock H 1974 *Solid State Commun.* **15** 1185
[19] Dunn A G, Jewess M, Staveley L A K and Worswick R D 1983 *J. Chem. Thermodyn.* **15** 351
[20] Igartua J M, Ruiz-Larrea I, Couzi M, Lopez-Echarri A and Breczewski T 1991 *Phys. Status Solidi* b **168** 67
[21] Gopal E S R 1966 *Specific Heat at Low Temperatures* (London: Heywood)
[22] Aguirre-Zamalloa G, Couzi M, Madariaga G, Lopez-Echarri A, Igartua J M and Breczewski T 1994 *Ferroelectrics* **156** 161
[23] Lopez-Echarri A, Ruiz-Larrea I and Tello M J 1990 *J. Phys.: Condens. Matter* **2** 513
[24] Samara G A, Peercy P S and Morosin B 1973 *Solid State Commun.* **13** 1525
[25] Gesi K 1986 *Ferroelectrics* **66** 269

[26] Shimizu H, Oguri A, Abe N, Yasuda N, Fujimoto S, Sawada S, Shiroishi Y and Takashige M 1979 *Solid State Commun.* **29** 125
[27] Aguirre-Zamalloa G, Madariaga G, Couzi M and Breczewski T 1993 *Acta Crystallogr.* B **49** 691
[28] Aguirre-Zamalloa G, Igartua J M, Couzi M and Lopez-Echarri A 1994 *J. Physique* I **4** 1237
[29] Aguirre-Zamalloa G, Couzi M, Chanh N B and Gallois B 1990 *J. Physique* **51** 2135
[30] Aguirre-Zamalloa G, Rodriguez V, Couzi M, Sayetat F and Fertey F 1997 *J. Phys.: Condens. Matter* **9** 937
[31] Braud M N, Couzi M and Chanh N B 1990 *J. Phys.: Condens. Matter* **2** 8243
[32] Couzi M, Negrier P, Poulet H and Pick R M 1988 *Croatica Chem. Acta* **61** 649
[33] Salje E K H 1990 *Phase Transitions in Ferroelastic and Co-elastic Crystals* (Cambridge: Cambridge University Press)
[34] Toledano J C and Toledano P 1987 *The Landau Theory of Phase Transitions* (Singapore: World Scientific)
[35] Jewess M 1982 *Acta Crystallogr.* B **38** 1418
[36] Bradley C J and Cracknell A P 1972 *The Mathematical Theory of Symmetry in Solids* (Oxford: Clarendon)
[37] Levola T and Laiho J 1986 *J. Phys. C: Solid State Phys.* **19** 6931
[38] Rodriguez V, Aguirre-Zamalloa G, Couzi M and Roisnel T 1995 *J. Phys.: Condens. Matter* **7** 1
[39] Huller A and Press W 1979 *The Plastically Crystalline State* ed J N Sherwood (Chichester: Wiley) p 345
[40] Couzi M and Aguirre-Zamalloa G 1997 in preparation
[41] Aguirre-Zamalloa G 1994 *PhD Thesis* University of Bordeaux I
[42] Gufan Y M and Larin E S 1980 *Fiz. Tverd. Tela* **22** 463
[43] Gufan Y M and Torgashev V I 1981 *Sov. Phys.–Solid State* **23** 656
[44] Salje E K H and Devarajan V 1986 *Phase Transitions* **6** 235